Electronic and Steric Factors in the Stability of a Protofullerene Framework: Indacenoid Isomers of $C_{30}H_{12}$

P. W. Fowler* and D. Mitchell

Department of Chemistry, University of Exeter, Stocker Road, Exeter, Devon, EX4 4QD, U.K.

Received May 1, 1995®

Semiempirical all-valence-electron calculations on the 45 indacenoid isomers of $C_{30}H_{12}$ show a strong correlation between low curvature and high overall stability, with topological π stabilization playing only a minor role. As with the fullerenes themselves, the energies of these protofullerene patches generally follow an isolated-pentagon rule, but a more important requirement for stability in the patch is that both pentagons should lie on its perimeter.

INTRODUCTION

Benzenoids and other polycyclic hydrocarbons have long been studied both for their intrinsic chemical interest and as a testing ground for qualitative models of electronic structure.[1,2] The advent of the fullerenes has revived interest in graph theoretical treatments of π systems[3] and in polycyclic carbon skeletons as possible fullerene precursors.[4,5] Ideas developed for one class of molecules are proving useful for the other. For example, the leapfrog construction for generating closed-shell fullerenes[6] has a counterpart that yields total-resonant sextet benzenoids,[7,8] and the concept of the Clar sextet[9] itself can be used to classify fullerenes[10] and rationalize their electron-deficient chemistry.[11] It is, however, risky to rely solely on π-electronic arguments for predicting fullerene isomer preference as "steric" and "electronic" contributions to the total energy are usually in fine balance.[3] The present paper seeks to apply current thinking on fullerene stability to polycyclic hydrocarbons with hexagonal and pentagonal rings, where curvature may be expected to play a significant role. The particular example chosen is the set of fused indacenoid (2-pentagon) hydrocarbons of formula $C_{30}H_{12}$, which were recently discussed in terms of π-electronic structure.[5] It will be shown that σ and π effects are strongly coupled in these molecules too, though with different consequences in the open indacenoid and closed fullerene frameworks. It will be suggested that, unfortunately, little can be deduced about the overall stability of indacenoids from Hückel calculations alone.

GRAPH THEORETICAL BACKGROUND

Dias has given a tabulation of constraints and equalities obeyed by polycyclic frameworks,[2] which can be used to show that the formula $C_{30}H_{12}$ admits 45 distinct fused polycyclic isomers, each having two pentagonal rings and all other rings hexagonal. A pair of enantiomers is counted here as a single distinct isomer. Pruned of hydrogen atoms, the skeletal graph of such an isomer has 10 internal trivalent vertices, 8 trivalent and 12 divalent vertices on the perimeter, 19 internal and 20 external edges, and 10 rings (= 2 pentagons and 8 hexagons). The full set of isomers is generated by systematically circumscribing the 13 possible 10-vertex excised internal structures listed in Figure 1 of ref 5. Graphs for each (including the CH bonds) are shown in our Figure 1.

Each graph is planar in the topological sense that it can be drawn without edges crossing in the plane, and each is described by a maximal[12] group (D_{2h} or one of the subgroups C_{2v}, C_{2h}, C_s). Physical realizations of the indacenoid graphs using realistic bond lengths and angles are all curved to a greater or lesser extent, and the physical point group is reduced from the maximal group by the removal of in-plane symmetry elements i.e., D_{2h} (maximal) → C_{2v} (physical), C_{2h} → C_2, C_{2v} → C_s, and C_s → C_1. As the correspondence is one-to-one, the indacenoid graphs can be classified without ambiguity using either group. The 45 indacenoids have maximal symmetries D_{2h} (4), C_{2v} (5), C_{2h} (2), and C_s (34).

Other useful invariants are as follows: N_P the number of pentagon fusions (0 or 1), N_{SW} the number of pyracylene (Stone−Wales) patches in which an edge links vertices of two distinct pentagons (0 or 1), and $\{\lambda_i\}$ the eigenvalue spectrum of the adjacency matrix. In particular the HOMO and LUMO eigenvalues are of interest. If the eigenvalues for an n electron system ($n = 30$ in this case) are arranged in descending order, then the eigenvalue of the HOMO is $\lambda_{n/2}$ and that of the LUMO is $\lambda_{n/2+1}$. The distinct types of π electronic configuration in Hückel theory are then open ($\lambda_{n/2} = \lambda_{n/2+1}$), properly closed ($\lambda_{n/2} \neq \lambda_{n/2+1}$, $\lambda_{n/2} > 0$, $\lambda_{n/2+1} \leq 0$), pseudo-closed ($\lambda_{n/2} \neq \lambda_{n/2+1}$, $\lambda_{n/2+1} > 0$), and meta-closed ($\lambda_{n/2} \neq \lambda_{n/2+1}$, $\lambda_{n/2} \leq 0$).[10] On this classification most fullerenes are pseudo-closed, but most benzenoids are properly closed. Amongst the 45 indacenoids of Figure 1 only **40** has an open-shell, **2**, **3**, **8**, **10**, **15**, and **16** are pseudo-closed, and the remaining 38 isomers are properly closed in simple Hückel theory (i.e., in the version of the model where all carbon atoms share a common α and all bonds a common β parameter independent of lengths and angles).

The HOMO−LUMO gaps Δ for the indacenoid graphs run from 0 $|\beta|$ (**40**) to 0.975 $|\beta|$ (**38**), and the delocalisation energies E_{RES} run from 0.433 $|\beta|$ (**40**) to 0.461 $|\beta|$ (**38**) per carbon atom. Neither Δ nor E_{RES} makes a sharp distinction between indacenoids with isolated and adjacent pentagons: **38** is the "best" isomer on both criteria and has isolated pentagons, but so does **2** which is the second worst isomer on both criteria; **44**, with adjacent pentagons has the sixth largest band gap and fourth largest delocalization energy.

® Abstract published in *Advance ACS Abstracts*, July 15, 1995.

0095-2338/95/1635-0874$09.00/0

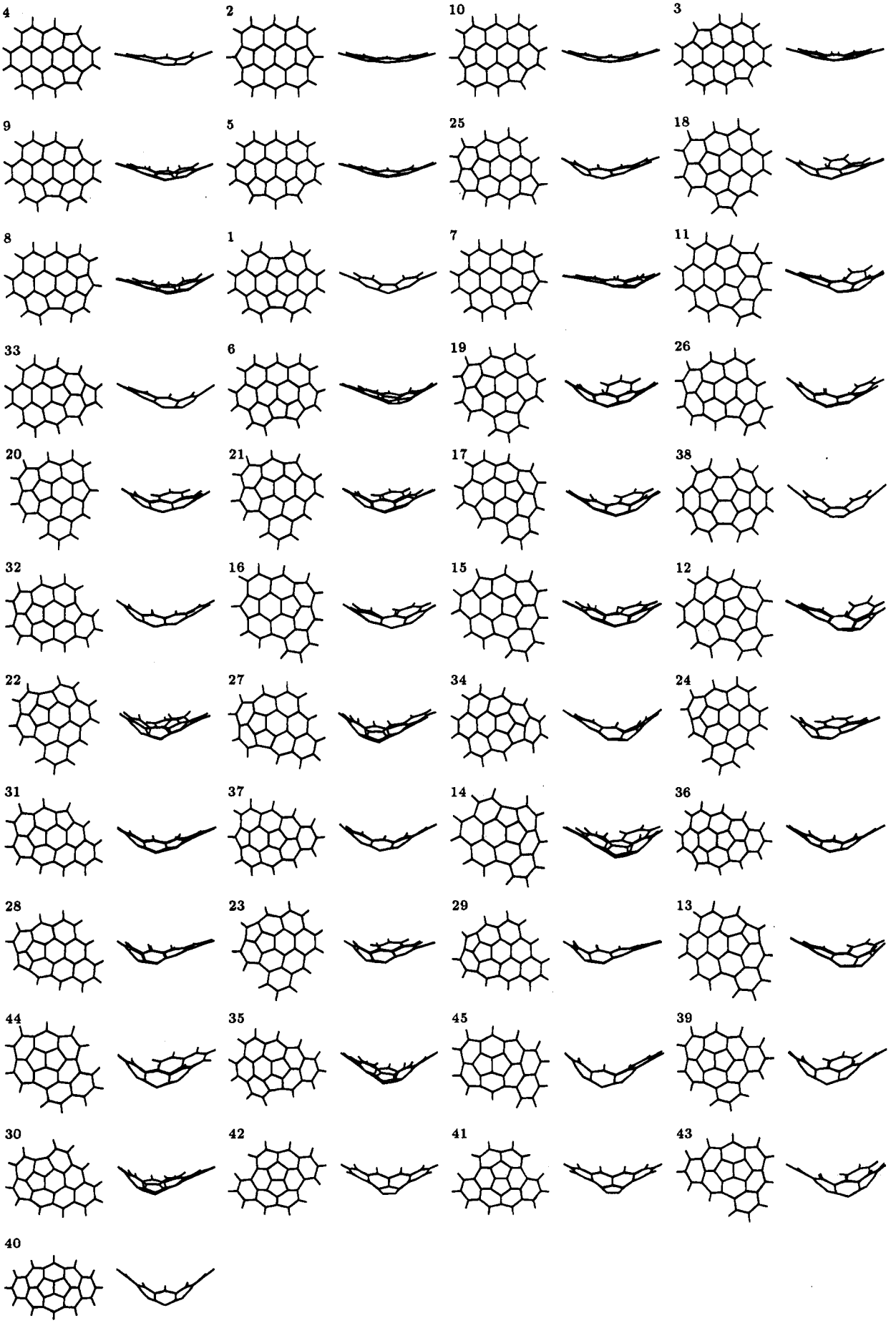

Figure 1. The 45 indacenoid isomers of $C_{30}H_{12}$. The diagrams are scale drawings of the optimized MNDO geometries and are listed in order of decreasing stability (see Table 1).

Table 1. Topological, Geometric, and Energetic Properties of the 45 Indacenoids of Formula $C_{30}H_{12}$[a]

isomer	symmetry	N_P	N_{SW}	E_{MNDO}/kJ mol^{-1}	$E_{RES}/\lvert\beta\rvert$	Δ_{MNDO}/eV	$\Delta_{HMO}/\lvert\beta\rvert$	ΔI
4	$C_{2v}(C_s)$	0	1	0.0	0.447	6.3	0.300	0.022
2	$D_{2h}(C_{2v})$	0	0	10.1	0.438	5.6	0.004	0.010
10	$C_s(C_1)$	0	0	18.0	0.444	5.5	0.199	0.015
3	$C_{2h}(C_2)$	0	0	18.7	0.446	5.3	0.319	0.019
9	$C_s(C_1)$	0	0	29.8	0.451	5.9	0.357	0.039
5	$C_{2v}(C_s)$	0	0	30.7	0.448	5.3	0.356	0.023
25	$C_s(C_1)$	0	0	36.6	0.452	6.3	0.621	0.051
18	$C_s(C_1)$	0	0	43.3	0.454	6.2	0.627	0.051
8	$C_s(C_1)$	0	1	43.8	0.448	5.7	0.186	0.037
1	$D_{2h}(C_{2v})$	0	1	47.3	0.457	6.2	0.488	0.064
7	$C_s(C_1)$	1	0	52.9	0.447	6.0	0.276	0.022
11	$C_s(C_1)$	0	1	75.7	0.451	6.1	0.409	0.059
33	$C_{2v}(C_s)$	0	1	79.2	0.452	6.5	0.690	0.072
6	$C_s(C_1)$	1	0	81.7	0.452	5.9	0.427	0.046
19	$C_s(C_1)$	0	1	107.0	0.459	6.6	0.682	0.086
26	$C_s(C_1)$	0	1	111.9	0.456	6.8	0.738	0.095
20	$C_s(C_1)$	0	0	114.9	0.452	6.2	0.449	0.066
21	$C_s(C_1)$	0	1	131.0	0.451	6.0	0.348	0.067
17	$C_s(C_1)$	0	1	142.1	0.449	6.1	0.319	0.078
38	$D_{2h}(C_{2v})$	0	1	151.2	0.461	7.2	0.975	0.118
32	$C_s(C_1)$	0	0	159.5	0.452	5.6	0.409	0.088
16	$C_s(C_1)$	0	0	162.9	0.448	5.8	0.327	0.067
15	$C_s(C_1)$	0	1	185.4	0.445	5.5	0.137	0.072
12	$C_s(C_1)$	1	0	218.0	0.457	6.1	0.537	0.096
22	$C_s(C_1)$	1	0	225.6	0.457	6.0	0.533	0.090
27	$C_s(C_1)$	1	0	226.5	0.454	6.2	0.534	0.101
34	$C_s(C_1)$	1	0	230.1	0.454	6.3	0.567	0.121
24	$C_s(C_1)$	1	0	234.9	0.450	5.6	0.376	0.066
31	$C_s(C_1)$	0	1	251.4	0.443	4.7	0.167	0.077
37	$C_{2v}(C_s)$	0	0	255.6	0.445	4.9	0.373	0.092
14	$C_s(C_1)$	1	0	266.4	0.454	5.7	0.386	0.101
36	$C_s(C_1)$	0	1	268.4	0.443	4.8	0.198	0.100
28	$C_s(C_1)$	1	0	271.5	0.446	5.7	0.365	0.061
23	$C_s(C_1)$	1	0	273.9	0.450	5.3	0.356	0.065
29	$C_s(C_1)$	1	0	278.4	0.445	5.6	0.298	0.059
13	$C_s(C_1)$	1	0	289.2	0.450	5.5	0.386	0.081
44	$C_s(C_1)$	1	0	295.8	0.457	6.4	0.627	0.133
35	$C_s(C_1)$	1	0	301.7	0.451	5.5	0.374	0.136
45	$C_s(C_1)$	1	0	306.3	0.454	6.4	0.560	0.145
39	$C_s(C_1)$	1	0	349.5	0.454	6.0	0.440	0.144
30	$C_s(C_1)$	1	0	356.7	0.449	4.8	0.259	0.095
42	$C_{2h}(C_2)$	1	0	373.6	0.453	5.6	0.393	0.152
41	$C_{2v}(C_s)$	1	0	376.4	0.453	5.7	0.401	0.145
43	$C_s(C_s)$	1	0	401.6	0.447	5.6	0.246	0.156
40	$D_{2h}(C_{2v})$	1	0	614.9	0.433	2.9	0.000	0.214

[a] The isomer numbering follows that of Figure 1. The symmetry entry lists the maximal (and actual) point groups; N_P and N_{SW} count pentagon adjacencies and pyracylene patches. E_{MNDO} is the heat of formation relative to the most stable isomer **4** (kJ mol^{-1}) and Δ_{MNDO} is the computed HOMO−LUMO gap (eV). E_{RES} is the Hückel delocalization energy per π electron of the molecular graph and Δ_{HMO} its HOMO−LUMO gap (both in units of $|\beta|$). ΔI is the dimensionless inertia defect, as defined in the text.

CALCULATIONS OF ELECTRONIC AND GEOMETRIC STRUCTURE

Geometries and total energies of all 45 isomers were compared using the semiempirical MNDO[13] method to include contributions from all valence electrons. This approach is economical and represents a reasonable compromise between the topological π-only model and a fully *ab initio* treatment; if its limitations are kept in mind it can be used to give a qualitatively correct account of the curvature of the σ framework and its effect on the π system. For each isomer the starting geometry was generated from scaled topological coordinates[12] based on the eigenvectors of the adjacency matrix, and full optimization was carried out for a closed-shell ground state. For isomer **40** Hückel theory predicts an open π shell, but this would presumably close under Jahn−Teller distortion: the closed-shell configuration has a HOMO−LUMO gap of only 2.9 eV, to be compared with the range of 4.7−7.2 eV of the other isomers. The results were checked for excessive dependence on the MNDO parameterization by rerunning all calculations in the PM3 model. Apart from some minor changes in order, the two sets of results are in close agreement, with a linear correlation (E_{PM3}/kJ mol^{-1}) = 0.898 (E_{MNDO}/kJ mol^{-1}) + 151 kJ mol^{-1} and a standard deviation of only 15 kJ mol^{-1} for the set of 45 data points.

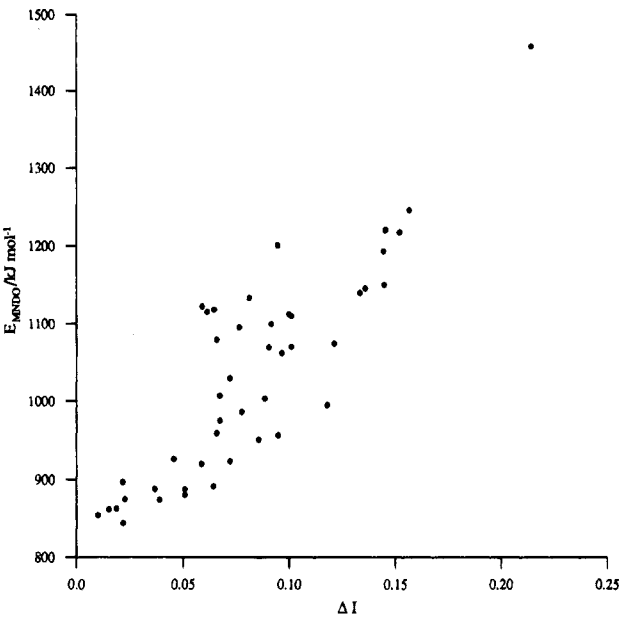

Figure 2. Correlation between stability (as computed in the MNDO model) and curvature (as measured by the dimensionless inertia defect of the MNDO structure) for the 45 indacenoids.

Every isomer gave rise to a local minimum on the MNDO potential energy surface (as checked by diagonalization of the Hessian for all but **40**). The lowest vibrational frequencies for the common ^{12}C, ^{1}H isotopomers range from 67 to 89 cm^{-1}. The calculated geometries are illustrated in plan and elevation in Figure 1, where they are listed in order of decreasing stability as measured relative to the most stable isomer, **4**, which has an absolute MNDO heat of formation of 844 kJ mol^{-1}. Topological and energetic properties of the 45 isomers are listed in Table 1.

The precise energy ordering should not be taken too literally. Several pairs of isomers are separated by only a few kJ mol^{-1}, and it is quite possible in such cases that a different method would reverse their relative stabilities. Where the gap is large, the prediction is firmer. Thus, **18** and **8** are essentially indistinguishable in MNDO stability, whereas no improvement in treatment is likely to predict **40** to be more stable than **38** or **38** more stable than **4**.

Several trends are evident in the energies. First, overall stability is strongly linked to curvature of the molecule; the flatter the profile of the isomer, the lower its computed energy. A numerical measure of curvature can be defined from the inertia defect, $\Delta I = (I_{cc} - I_{bb} - I_{aa})/I_{cc}$, where $I_{aa} \le I_{bb} \le I_{cc}$ are the moments of inertia of the molecule about its principal axes and ΔI would vanish for a planar system. This measure is listed in Table 1 and is used to quantify the correlation between stability and curvature in Figure 2.

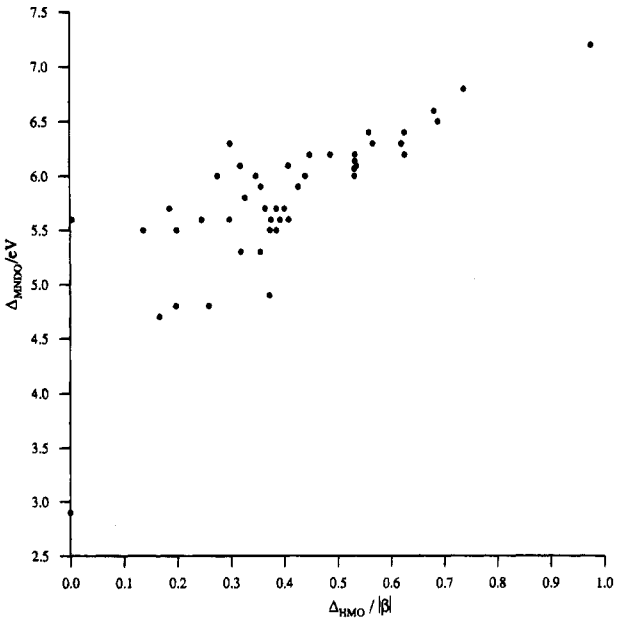

Figure 3. Correlation between computed (MNDO) and graph-theoretical (Hückel) HOMO−LUMO gaps for the 45 indacenoids. The outlier at $\Delta_{HMO} = 0$ is isomer **40**, which has a closed-shell ground state in the MNDO approximation, as discussed in the text.

Curvature is intimately linked with the positions of the pentagons within the patch of fused rings, and in general the most stable isomers are those with isolated pentagons ($N_P = 0$). Twenty-one of 24 isolated pentagon isomers occur in the 23 most stable structures, and the first isomer with adjacent pentagons lies 53 kJ mol^{-1} above the best structure. Isomers where pentagons lie on the periphery are preferred over those where both lie within the patch, even to the extent that **7** with adjacent pentagons but where both are on the periphery is predicted to be more stable than 14 of the 16 isomers that have isolated pentagons but with one or both embedded in the patch. Peripheral pentagons allow the molecule to have a mainly flat graphitic structure with some curling up at the edges, whereas embedded pentagons produce a more highly curved bowl shape. This route for minimizing curvature is not available to the fullerenes, where graphitization of hexagons on one part of the surface implies crowding of pentagons and sharp curvature elsewhere.[14]

A second feature of interest is the generally good correlation between the HOMO−LUMO gap computed in MNDO and Hückel models (Figure 3). Although Hückel theory is a good predictor of this frontier-orbital property, the gap is not well correlated with overall stability. The picture that this suggests is one where curvature of the framework leads to reduction of π overlap and damping of the π energy.

Perhaps the most significant trend is the lack of correlation between overall stability and Hückel predictions. The 45 isomers span a range of over 600 kJ mol^{-1}, and the isomer with the largest HOMO−LUMO gap and highest π delocalization energy[5] in the crude Hückel model (the D_{2h} "circofulvalene"[5] or "buckybowl"[15] isomer **38**) lies only 20th in order of stability according to the MNDO calculations, some 150 kJ mol^{-1} above the much flatter **4**. π energies appear to have a secondary role in overall stability but can lead to occasional switches in the order that would be expected on grounds of curvature alone. For example, **2** is apparently less curved ($\Delta I = 0.010$) than **4** ($\Delta I = 0.022$) but has a nearly vanishing HOMO−LUMO gap, whereas **4** has a separation of 0.300 $|\beta|$ in the planar Hückel model; in the event **2** is predicted to be less stable than **4** by 10 kJ mol^{-1}. Similarly the large gap of 0.975 $|\beta|$ for **38** appears to moderate the effect of its substantial curvature ($\Delta I = 0.118$). The poor showing of isomer **38** in the energy ranking is perhaps surprising, as it is the only (D_{2h}) isomer of $C_{30}H_{12}$ to have been synthesized so far.[5,15] The fact that a $C_{30}H_{12}$ can be assembled in a stepwise synthesis is not, of course, conclusive proof that it lies at the global minimum of the potential energy surface; the most stable arrangement of 30 carbon and 12 hydrogen atoms is unlikely to be an indacenoid at all as all of these molecules have large, positive standard heat of formations.

Curvature also correlates with rigidity of the indacenoid framework. An upper bound for the activation energy for bowl-to-bowl inversion can be obtained by reoptimizing the geometry while enforcing planarity. The barrier heights estimated in this way for the five most stable isomers range from 5.2 to 76 kJ mol^{-1} (MNDO). Isomers with more curvature, **19** and **38**, have estimated activation energies of 308 and 312 kJ mol^{-1}, respectively. Inversion of any one of five *least* stable isomers is estimated to require at least 600 kJ mol^{-1}. Corannulene, $C_{20}H_{10}$, is known to undergo rapid inversion at room temperature and has a likely barrier height[16] of ~50 kJ mol^{-1}.

Inversion interconverts enantiomers. A hypothetical mechanism for more general isomerization that has been much discussed in the context of fullerenes is the Stone−Wales transformation.[17] Rotation of the central bond of a pyracyclene patch coverts its two pentagons to hexagons and *vice versa*, allowing pentagons to move around on the surface of the fullerene cage. A Stone−Wales bond has a characteristic site symmetry (C_{2v} or a subgroup) that is preserved during the rearrangement, but for fullerenes the overall molecular symmetry is normally changed, allowing generation of chiral fullerenes from achiral parents and so on.

Amongst the 45 indacenoids there are 13 with $N_{SW} = 1$ and for these the site symmetry of the pyracyclene patch must coincide with the point group of the molecule, so that reactant and product isomers must share a common point group and no achiral indacenoid can become chiral by this mechanism. The interconnecting pairs are **1** ↔ **38** (C_{2v}), **4** ↔ **33** (C_s), **15** ↔ **21** (C_1), **8** ↔ **11** (C_1), **17** ↔ **26** (C_1), **31** ↔ **36** (C_1) and **19** ↔ **19** (C_1). The transformation of **19** connects its left and right forms and is thus equivalent to bowl-to-bowl inversion for this structural isomer.

Dias[5] argues that the transformation **1** ↔ **38** should be facile because these isomers share 17 out of 30 Hückel eigenvalues in common, and therefore the isomerization would be accompanied by the minimum of electronic reorganization. In contrast, the MNDO energies suggest that 104 kJ mol^{-1} would be needed to climb from **1** to **38** even if the transformation occurred without a barrier, which is more than would be needed for any of the other SW pairs. The barrier to the transformation in fullerenes is thought to be high (e.g., of the order of 500−600 kJ mol^{-1} [18−20]). More generally, no correlation appears to exist between similarity of Hückel eigenvalue spectra for a pair of indacenoids and their relative stability in the MNDO model.

CONCLUSION

This study of overall stabilities within a complete set of isomeric indacenoid hydrocarbons suggests the following conclusions.

(1) Curvature strain plays the dominant role in overall stability for non-benzenoid polycyclic hydrocarbons as for fullerenes.

(2) The rules of thumb for minimizing steric strain are however different for these indacenoids and fullerenes. For indacenoids, isolation of pentagons is stabilizing, but it is more important to have the two pentagons on the perimeter of the fused network. For fullerenes, there is no perimeter, and pentagon-isolation is the first prerequisite for stability. Protofullerene patches with more pentagons or with more outer layers of hexagons may be closer to fullerenes in this respect.

(3) As with the fullerenes themselves, it does not appear to be possible to predict relative stabilities of indacenoids reliably from simple Hückel arguments. The lack of correlation between MNDO stability and MNDO band gap suggests that it would not be enough to modify the topological model of π-electronic structure to take curvature into account. The σ electrons have an important role in stability.

REFERENCES AND NOTES

(1) Knop, J. V.; Müller, W. R.; Szymanski, K.; Trinajstić, N. *Computer Generation of Certain Classes of Molecules*; SKTH: Zagreb, 1985.

(2) Dias, J. R. *Handbook of Polycyclic Hydrocarbons, Parts A and B*; Elsevier: Amsterdam, 1987/1988.

(3) Fowler, P. W.; Manolopoulos, D. E. *An Atlas of Fullerenes*; Oxford University Press: Oxford, 1995.

(4) Taylor, R.; Langley, G. J.; Kroto, H. W.; Walton, D. R. M. *Nature* **1993**, *366*, 728.

(5) Dias, J. R. *J. Chem. Inf. Comput. Sci.* **1995**, *35*, 148.

(6) Fowler, P. W.; Steer, J. I. *J. Chem. Soc.* **1987**, 1403.

(7) Dias, J. R. *Chem. Phys. Lett.* **1993**, *204*, 486.

(8) Fowler, P. W.; Austin, S. J.; Dunning, O. J.; Dias, J. R. *Chem. Phys. Lett.* **1994**, *224*, 123.

(9) Clar, E. *Polycyclic Hydrocarbons*; Academic: London, 1964.

(10) Fowler, P. W.; Pisanski, T. *J. Chem. Soc., Faraday Trans.* **1994**, *90*, 2865.

(11) Fowler, P. W.; Ceulemans, A. *J. Phys. Chem.* **1995**, *99*, 68.

(12) Manolopoulos, D. E.; Fowler, P. W. *J. Chem. Phys.* **1992**, *96*, 7603.

(13) The calculations used MOPAC 6.00: Stewart, J. J. P. *Quantum Chemistry Program Exchange*, Department of Chemistry, Indiana University, Bloomington, Indiana, 47405 U.S.A.

(14) Austin, S. J.; Fowler, P. W.; Manolopoulos, D. E.; Orlandi, G.; Zerbetto, F. *J. Chem. Phys.* **1995**, *99*, 8076.

(15) Rabideau, P. W.; Abdourazak, A. H.; Folsom, H. E.; Marcinow, Z.; Sygula, A.; Sygula, R. *J. Am. Chem. Soc.* **1994**, *116*, 7891.

(16) Sygula, A.; Rabideau, P. W. *J. Chem. Soc., Chem. Commun.* **1994**, 1497.

(17) Stone, A. J.; Wales, D. J. *Chem. Phys. Lett.* **1986**, *128*, 501.

(18) Baker, J.; Fowler, P. W. *J. Chem. Soc., Perkin Trans. 2* **1992**, 1665.

(19) Yi, J. Y.; Bernholc, J. *J. Chem. Phys.* **1992**, *96*, 8634.

(20) Murry, R. L.; Strout, D. L.; Odom, G. K., Scuseria, G. E. *Nature* **1993**, *366*, 665.

CI950042K